Direct Measurement of Reaction Kinetics for the Decomposition of Ultrathin Oxide on Si(001) Using Scanning Tunneling Microscopy

K. E. Johnson[(a)] and T. Engel

Department of Chemistry BG-10, University of Washington, Seattle, Washington 98195

(Received 18 February 1992)

The spatially inhomogeneous thermal decomposition of monolayer thick oxide films on Si(001) has been investigated. After partial desorption, uniformly distributed voids are formed in the oxide layer. Analysis of the evolution in the void area distribution with extent of desorption suggests that the rate determining step in void growth is the creation of a diffusing Si monomer within the void. This explains the unexpected substantial rearrangement of the Si substrate upon desorption of a single monolayer of oxygen.

PACS numbers: 68.55.Jk, 82.65.Yh

Both thick [1] and ultrathin [2,3] oxide films on silicon decompose thermally with spatial inhomogeneity, yielding SiO as the reaction product. These voids which expose the clean silicon substrate grow laterally as the reaction proceeds without a thinning of the remaining oxide film. Still to be understood are the atomic level reaction pathways which lead to void formation and growth. We have used scanning tunneling microscopy (STM) to directly follow the thermal decomposition of an oxide film for the first time. Our study addresses the following questions. Are there preferential sites for void nucleation? Does the reaction proceed through a unimolecular step at the void perimeter? Can a one-monolayer-thick film be removed without substantial rearrangement of the substrate in what has been referred to as monolayer peeling?

This work was performed in a dual chamber ultrahigh vacuum STM system. Complete details of the apparatus appear elsewhere [4]. Vacuum preparation followed typical procedures for silicon STM imaging [5]. Vacancy densities for well-annealed samples were below 4%.

Oxide films were formed by exposure to 1×10^{-5} Torr sec of O_2 at 300 K. Coverage calibration with Auger electron spectroscopy (AES) was carried out using water adsorption on Si(001) [6]. [A 1-ML (monolayer) coverage is defined here as one oxygen atom per surface silicon atom.] We partially desorb SiO by controlled heating to 1000 K where the desorption reaction is slow enough to be interrupted by radiatively quenching the sample after 15–20 sec. The sample was transferred between heating stage and STM for imaging, so it was not possible to return to the same location after additional desorption. This procedure was repeated until the cumulative heating time desorbed all the remaining oxide. Reported here are only results for an initial 1.0 ± 0.1 ML oxygen coverage. However, the conclusions which we draw are also valid for coverages as low as 0.3 ML. All images were taken at 300 K using the constant current mode and are displayed in a height keyed gray scale.

Our STM images of Si(001) samples prior to oxidation show the (2×1) dimer-row reconstruction, with local step orientations which produced the expected alternating smooth and rough step edges. An image of a Si(001) surface before and after adsorption of 1 ML of oxygen is displayed in Fig. 1. Two substrate steps of height 1.36 Å are visible in Fig. 1(b), showing that the long-range order of alternating step height seen in Fig. 1(a) is still present although the adlayer exhibits no long-range order. Small granular features with apparent mean height of 1.1 ± 0.2 Å and mean diameter of 11 ± 2 Å are present at a density of 0.05 ML. No trace of the (2×1) reconstruction characteristic of the clean surface can be seen.

Desorption proceeds by the formation of voids in the oxide layer exposing clean silicon. Figure 2(a) shows an image taken after 13% of the oxygen was removed. Voids can be identified as the small dark features which are randomly nucleated on terraces. The remaining oxide ap-

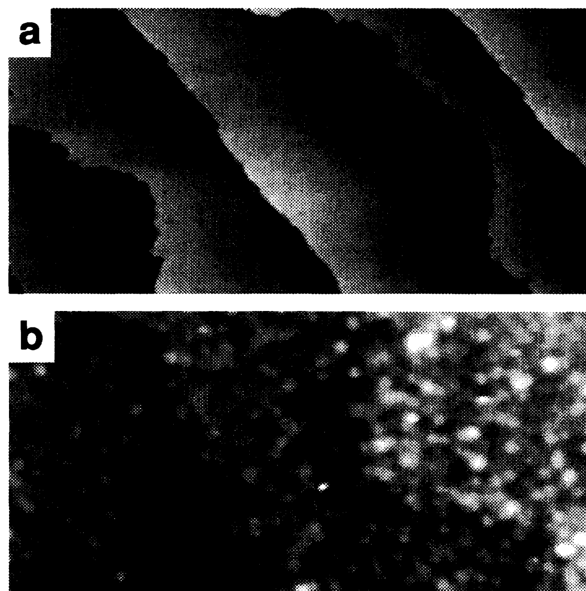

FIG. 1. (a) Image of Si(001) before adsorption. $V_{sample} = -2$ V and $I_{tunnel} = 1$ nA. Image size $\approx 4000\times2000$ Å. (b) Image of Si(001) with 1 ML oxygen. $V_{sample} = -4$ V, and $I_{tunnel} = 1$ nA. Image size $\approx 500\times250$ Å.

© 1992 The American Physical Society

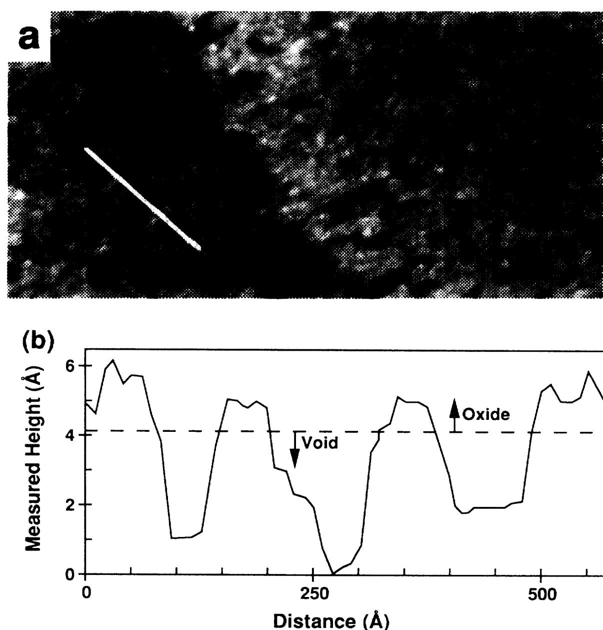

FIG. 2. (a) 2000×1000 Å image after 13% desorption of an initial 1 ML coverage. $V_{\text{sample}} = -4$ V and $I_{\text{tunnel}} = 1$ nA. (b) Line scan through the region indicated in (a). The left and right voids are two atomic layers deep whereas the middle void is three layers deep.

pears disordered as before. The presence of substrate step edges confirms that the underlying structure is preserved to this stage of desorption. A line scan through the region indicated in Fig. 2(a) is shown in Fig. 2(b). The dashed line distinguishing oxide from substrate is established using high-resolution scans which easily distinguish between disordered oxide and the $p(2\times 1)$ Si found in the voids. The oxide height is uncertain since we have not determined the barrier height difference for the clean and oxygen covered surface. Since the void edges can easily be located in such a line scan, void perimeters and areas can be assigned to each void and distributions characteristic of an ensemble of voids can be determined for images such as Fig. 2(a). This is important for the quantitative analysis to be presented below. The progress of the desorption reaction is estimated from the measured total void area. The void density decreases slightly after 13% desorption. This implies that once desorption initiates, no new voids are nucleated, and that by 13% desorption, voids have already begun to coalesce.

In the final stages of desorption the surface morphology will reflect more clearly the mechanism by which the oxide is removed. Figures 3(a) and 3(b) were imaged with $\approx 1\%$ oxide remaining. The surface is now roughened such that the step edges seen in Fig. 1 are obscured by pitting. The higher-resolution image in Fig. 3(b) shows localized disordered regions of oxide remaining on the highest level of silicon, and pitting up to five atomic layers deep. The substrate step structure is no longer apparent. All samples with > 75% oxide removed show extensive roughening. Removal of all of the oxygen at 1000 K results in the image seen in Fig. 3(c). Both SiO desorption and Si diffusion occur at this temperature. The substrate step structure initially present in the clean and the surface oxidized at 300 K reappears in a very disordered form. The length along the smooth and rough terrace edges has increased by factors of 1.3 and 2.0, respectively, relative to the surface before oxygen adsorption [4]. This is inconsistent with a model in which SiO desorption removes silicon from only the uppermost atomic layer as would be the case for monolayer peeling.

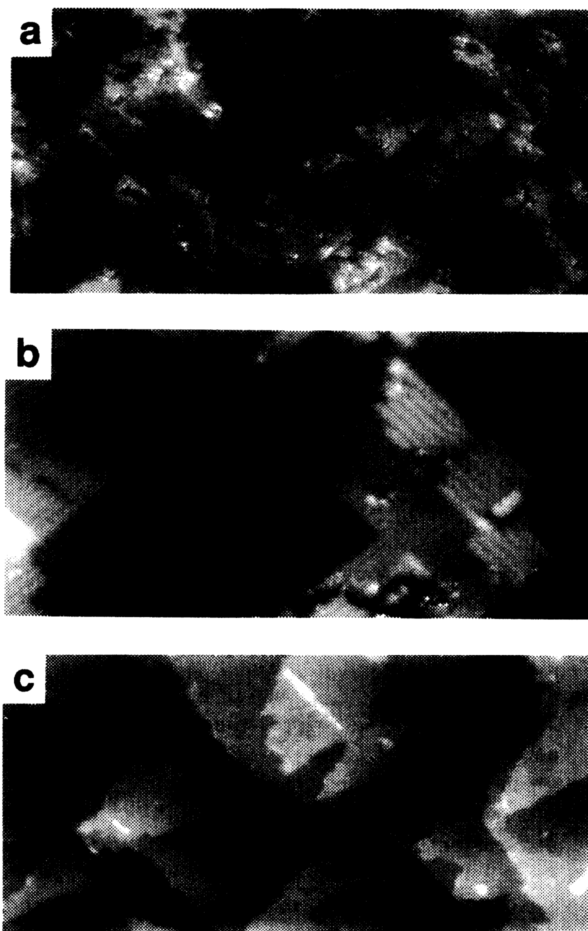

FIG. 3. (a),(b) Nearly complete desorption with $\approx 1\%$ of initial 1 ML remaining. $V_{\text{sample}} = -2$ V and $I_{\text{tunnel}} = 1$ nA. (a) Image size $\approx 1700\times 850$ Å. (b) Image size $\approx 425\times 215$ Å. (c) Image after complete removal of oxide at 1000 K. $V_{\text{sample}} = -2$ V and $I_{\text{tunnel}} = 1$ nA. Image size $\approx 4000\times 2000$ Å.

In order to model the kinetics of the void growth we consider the following simplified models to represent void growth after nucleation has taken place:

$$\mathrm{Si}(L) \underset{k_2}{\overset{k_1}{\rightleftarrows}} \mathrm{Si}(m)\,, \qquad (1)$$

$$\mathrm{Si}(m) \underset{k_4}{\overset{k_3}{\rightleftarrows}} \mathrm{Si}(P)\,, \tag{2}$$

$$\mathrm{Si}(P) + \mathrm{O}(P) \xrightarrow{k_5} (\mathrm{SiO}_x)\,, \tag{3}$$

$$(\mathrm{SiO}_x) \xrightarrow{k_6} \mathrm{SiO}(g)\,. \tag{4}$$

Si(L), Si(m), and Si(P) represent lattice silicon, a diffusing silicon monomer, and a monomer at the void perimeter, respectively. (SiO_x) represents a reactive site at the void perimeter which involves both silicon and oxygen in an unknown stoichiometric ratio. SiO(g) represents a gas phase SiO molecule.

As void growth is observed, the last step must occur. We have no *a priori* evidence that the kinetic steps of Eqs. (1)-(3), in which Si(m) is implicated in SiO(g) production, occur. If Si(m) is not involved, the reaction rate is described by Eq. (4). It will be proportional to $A^{1/2}$, where A is the area of an individual void since for the small degree of desorption which we consider, the perimeter is to a good approximation proportional to $A^{1/2}$. If Si(m) is involved, two limiting cases apply. If the reaction of Eq. (3) is rate limiting, all other steps are fast, and we assume a steady-state value for SiO_x, the reaction rate will be proportional to $A^{1/2}$. If the rate of formation of Si(m) is rate limiting, and the following steps are fast, the reverse rates in Eqs. (1) and (2) can be neglected. Since the rate of Si(m) production is proportional to the number of Si atoms in the void, the void growth rate will be proportional to $A^{1.0}$.

A distinction between the relative rates of these processes can be made if the functional dependence of $\partial A/\partial t$ on A can be determined. In our experiments, we have measured the distribution of void areas for an average total void area of 1.5%, 8%, and 13%. We can fit the distributions well by a function of the form $\rho_{\mathrm{void}}(A) = \xi/A^{\sigma}$. The data and the fits are shown in Fig. 4. We cannot determine $A(t)$ directly. However, we can obtain the same information by measuring the distribution of void areas for two differing values of the total amount desorbed. We determine the functional dependence of A on t by propagating the distribution for 1.5% desorption forward in time using $\partial A/\partial t = k'A^{\alpha}$ with $\alpha = 0.5$ and 1.0. The propagated curves for 8% and 13% desorption are then fitted by this equation and ξ and σ are extracted. These values can be compared with the values of ξ and σ determined directly from the experimental data. The dashed and solid lines in the inset of Fig. 4 show the expected dependence of ξ and σ on the extent of desorption for $\alpha = 0.5$ and 1.0. The experimental values are also shown. It is seen that the data agree quite well with the model for $\alpha = 1.0$ whereas poor agreement is obtained for $\alpha = 0.5$.

These results suggest that the creation of Si(m) is rate determining. If the equilibrium of Eq. (1) were established, surface defects should be rapidly healed by diffusion. This is not consistent with the deep etch pits clearly seen in Fig. 3. However, if the formation of Si(m) is rate determining, such etch pits would be predicted since monomers will be formed most readily at sites of low coordination number. If these are rapidly reacted away at the void perimeter to form SiO(g), etch pits will grow as we observe.

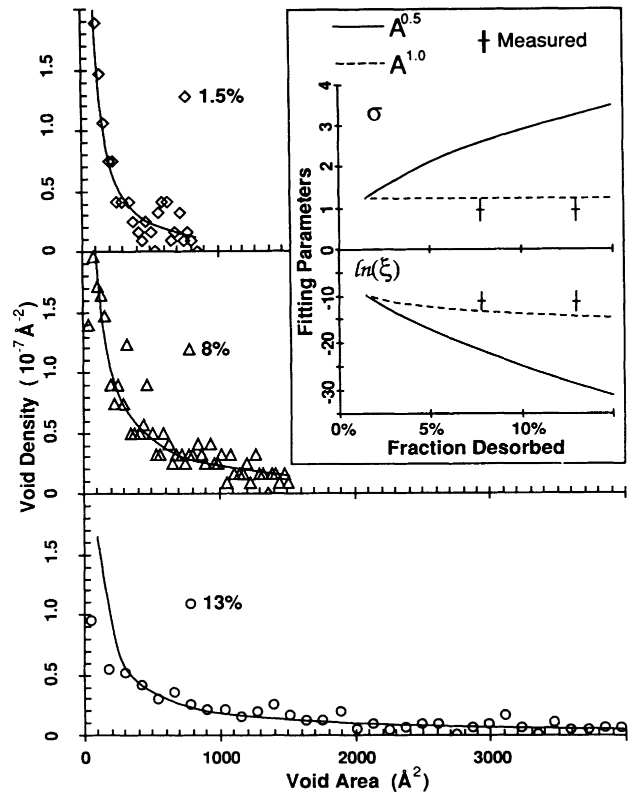

FIG. 4. Distributions of void areas for increasing desorption. Curves are fits by an inverse power law described in text. Inset: Comparison of the experimental and calculated parameters with two limits of the kinetic model. Vertical bars represent 95% confidence limits.

The surprising result that Si atoms within the void are needed to desorb SiO does not necessarily mean that the oxygen desorbs together with the diffusing silicon atom. The Si(m) may rather be needed to form a perimeter complex which breaks up more easily. These results explain why monolayer peeling of the ultrathin oxide layer does not occur and why after removal of the oxygen, considerable substrate rearrangement is seen.

Our model suggests that the rate determining step is the formation of a mobile Si monomer. Thermal desorption studies [3] have found that the activation energy for SiO(g) formation, E_a^{des}, is in the range of 3.2 to 3.6 eV. Simulations of Si diffusion on Si(100) [7,8] are consistent with such a large energy for promotion from a lattice site in the surface to a diffusing monomer. These studies also find an activation energy of 0.75 eV for diffusion, E_a^{diff},

and predict that diffusion will be highly anisotropic. The large discrepancy between E_a^{des} and E_a^{diff} as well as the much lower anisotropy in void shape which we see compared with Si island growth [9] support our contention that diffusion of Si cannot be rate determining for void growth.

The dependence of the void growth rate on the extent of desorption has been investigated in three previous experiments. Sun, Bonser, and Engel [2,3] determined E_a^{des} from thermal decomposition experiments for a model in which Eq. (3) is the rate determining step. However, they could only carry out measurements between 20% and 40% desorption where the void shapes are complex. Liehr, Lewis, and Rubloff [1] found that the void diameter in a 95-Å oxide film increased linearly in time for diameters in the range 2–80 μm. Because of the thick SiO_2 film formed, these authors measured the rate of the reaction $SiO_2 + Si \rightarrow 2SiO(g)$. In our experiment the low oxygen coverage ensures that the surface stoichiometry is the same as that of the gas phase product. Another STM study [10] was carried out for an intermediate film thickness of 12 Å, corresponding to about 5 ML. Up to 50% of the oxygen was desorbed, after which the samples were exposed to air and analyzed with STM. Since the samples were exposed to air before analysis and the distribution in void areas was not reported, no direct comparison can be made with our work.

In conclusion, we have found that void nucleation occurs randomly and monolayer peeling does not occur in the desorption of ultrathin oxide films on Si(100). By analyzing void area distributions as a function of the extent of desorption, we believe we have found an explanation of this behavior. The rate limiting step is not the perimeter reaction in which an oxygen atom and the silicon in the topmost layer are desorbed in a concerted step. Rather, the creation of a mobile silicon monomer which quickly reacts at a perimeter site to form $SiO(g)$ is the slow step in the kinetics. This explains the extensive roughening of the substrate which we observe upon SiO desorption. Comparison of our work to previous related work indicates that the void formation kinetics will depend sensitively on the nature of the oxide formed and its thickness. Studies such as these for oxide films of different thickness would provide further details of this important reaction.

Support for this work was provided by the Office of Naval Research and the Washington Technology Center.

---

[a]Present address: IBM Almaden Research Center, San Jose, CA 95120-6099.

[1] M. Liehr, J. E. Lewis, and G. W. Rubloff, J. Vac. Sci. Technol. A **5**, 1559 (1987); G. W. Rubloff, J. Vac. Sci. Technol. A **8**, 1853 (1990).

[2] Y.-K. Sun, D. J. Bonser, and T. Engel, Phys. Rev. B **43**, 14309 (1991).

[3] Y.-K. Sun, D. J. Bonser, and T. Engel, J. Vac. Sci. Technol. A (to be published).

[4] K. E. Johnson, P. Wu, M. Sander, and T. Engel (to be published).

[5] B. S. Swartzentruber, Y.-W. Mo, M. B. Webb, and M. G. Lagally, J. Vac. Sci. Technol. A **7**, 2901 (1989).

[6] D. Schmeisser, Surf. Sci. **137**, 197 (1984); W. Ranke and Y. R. Xing, Surf. Sci. **157**, 339 (1985).

[7] D. Srivastava and B. J. Garrison, J. Chem. Phys. **95**, 6885 (1991).

[8] Z. Zhang, Y. Lu, and H. Metiu, Surf. Sci. **248**, L250 (1991).

[9] Y.-W. Mo, J. Kleiner, M. B. Webb, and M. G. Lagally, Phys. Rev. Lett. **66**, 1998 (1991).

[10] Y. Kobayashi and K. Sugii, J. Vac. Sci. Technol. B **9**, 748 (1991).

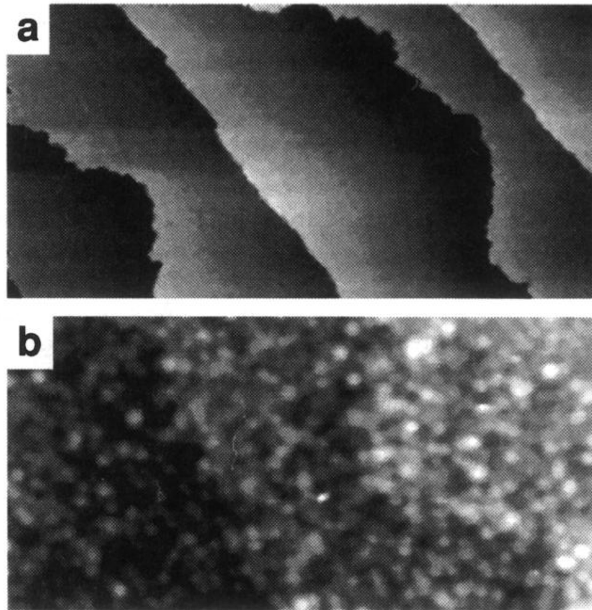

FIG. 1. (a) Image of Si(001) before adsorption. $V_{sample} = -2$ V and $I_{tunnel} = 1$ nA. Image size $\approx 4000 \times 2000$ Å. (b) Image of Si(001) with 1 ML oxygen. $V_{sample} = -4$ V, and $I_{tunnel} = 1$ nA. Image size $\approx 500 \times 250$ Å.

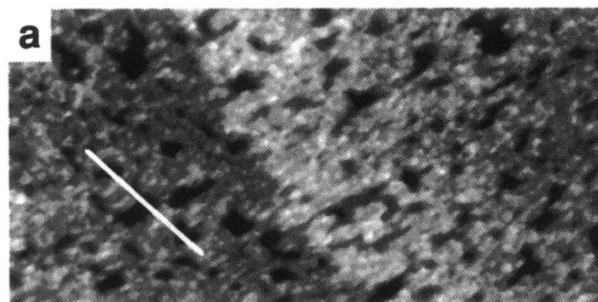

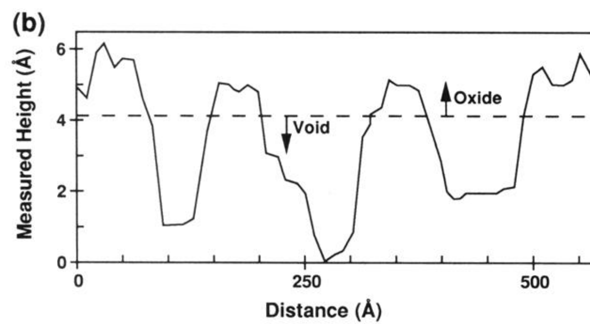

FIG. 2. (a) 2000×1000 Å image after 13% desorption of an initial 1 ML coverage. $V_{\mathrm{sample}}=-4$ V and $I_{\mathrm{tunnel}}=1$ nA. (b) Line scan through the region indicated in (a). The left and right voids are two atomic layers deep whereas the middle void is three layers deep.

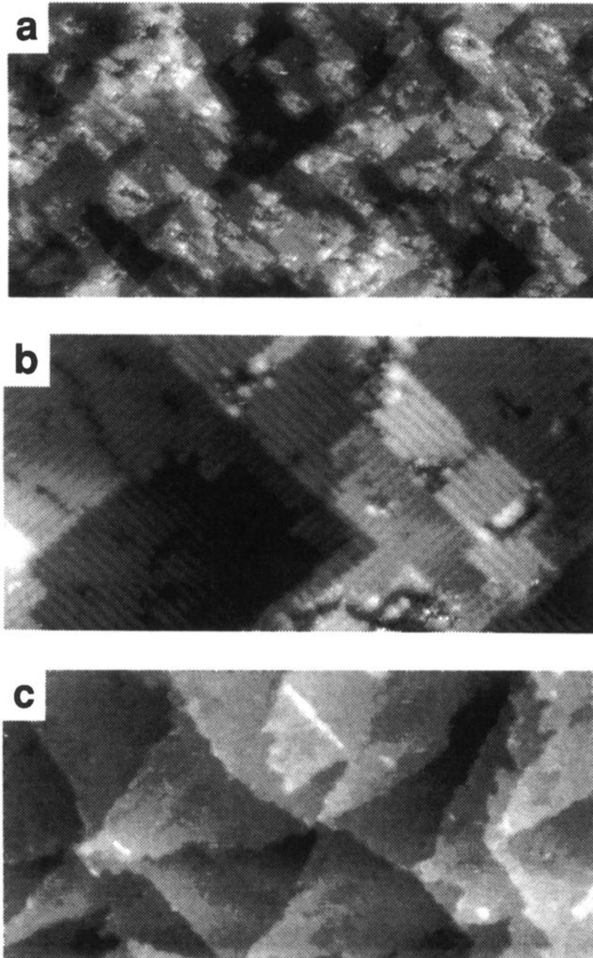

FIG. 3. (a),(b) Nearly complete desorption with $\approx 1\%$ of initial 1 ML remaining. $V_{\text{sample}} = -2$ V and $I_{\text{tunnel}} = 1$ nA. (a) Image size $\approx 1700 \times 850$ Å. (b) Image size $\approx 425 \times 215$ Å. (c) Image after complete removal of oxide at 1000 K. $V_{\text{sample}} = -2$ V and $I_{\text{tunnel}} = 1$ nA. Image size $\approx 4000 \times 2000$ Å.